JOURNAL
OF THE AMERICAN CHEMICAL SOCIETY

VOLUME 93, NUMBER 13 JUNE 30, 1971

Physical and Inorganic Chemistry

Partitioning and Characterization of Molecular Charge Distributions

R. F. W. Bader,*[1a] P. M. Beddall,[1a] and P. E. Cade[1b]

Contribution from the Department of Chemistry, McMaster University, Hamilton, Ontario, and the Department of Chemistry, University of Massachusetts, Amherst, Massachusetts 01002.
Received September 8, 1970

Abstract: A partitioning of the total molecular charge distribution between the nuclei in a molecule is proposed. The method may be termed a "natural partitioning," as it is suggested by the nature of the charge distribution itself; the point along the internuclear axis at which the charge density attains its minimum value between a pair of bonded nuclei defines the position of the partitioning surface. The resulting populations are further divided into nonbonded and bonded populations for a terminal nucleus and into two bonded populations for a nucleus with two adjacent nuclei. These charge populations together with their associated nonbonded and bonded radii are sufficient to classify and characterize a molecular charge distribution. The variations in these parameters serve to summarize in a concise manner the type and variation in the type of bonding through isoelectronic series of molecules and through series of oxides, fluorides, etc., in ground, excited or charged states. A corresponding partitioning of molecular properties is illustrated in terms of the dipole moment, and the general inadequacy of this moment in providing a measure of the charge transfer within a system is discussed. Finally, the transferability of these bonded and nonbonded populations between different bonding environments (a necessary condition for the transferability of molecular properties) is illustrated and discussed.

There is a history of attempts to predict the distribution of electronic charge within a molecule and to partition the total electronic charge between the nuclei in the system. The prime reason for proposing any scheme which assigns some number of electrons to each nucleus in a molecule is to provide a measure of the charge transfer which has occurred on the formation of the molecule from the separated atoms. It is on such information that our present classification of the bonding in a system as ionic, polar, covalent, etc., is founded.[2-4]

The availability of electronic wave functions to Hartree–Fock accuracy, or beyond, permits one to calculate with considerable chemical accuracy the distribution of electronic charge in three-dimensional space.[5,6] A complete knowledge of the spatial distribution of the charge density implies a complete knowledge of all the physically meaningful properties which can be associated with it,[7] and hence in one sense the history of attempts to predict the distribution of charge within a molecule is complete. However, the availability of complete charge distributions has made the need for a classification scheme ever more pressing. Even a spatial display of a molecular charge distribution in the form of a contour map contains a wealth of detailed information, and there is a need for some set of parameters which will characterize the important properties of a charge distribution. It is the purpose of this work to provide such a set of parameters. The parameters should provide a measure both of the degree of transfer

(1) (a) McMaster University; (b) University of Massachusetts.
(2) (a) L. Pauling, "The Nature of the Chemical Bond," 3rd ed, Cornell University Press, Ithaca, N. Y., 1960, (b) R. S. Mulliken, *J. Chem. Phys.*, **23**, 1833 (1955).
(3) K. Ruedenberg, *Rev. Mod. Phys.*, **34**, 326 (1962).
(4) P.-O. Löwdin, *J. Chem. Phys.*, **21**, 374 (1953).
(5) C. W. Kern and M. Karplus, *ibid.*, **40**, 1374 (1964).
(6) G. G. Hall, *Phil. Mag.*, **6**, 249 (1961).
(7) P. Hohenberg and W. Kohn, *Phys. Rev.*, **136**, B864 (1964).

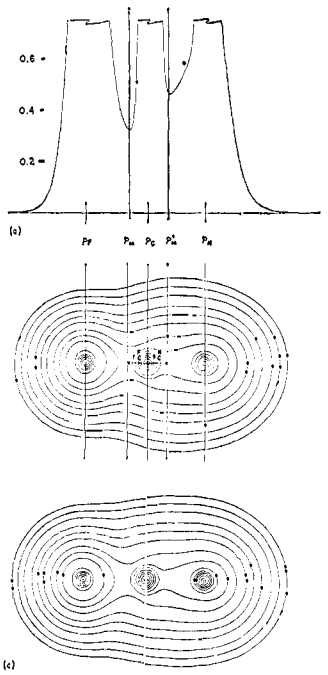

Figure 1. The positioning of the partitioning planes P_m and P_A for the charge distribution of FCN($X^1\Sigma^+$) (a) in profile along the internuclear axis and (b) in the plane containing the nuclei. (c) Charge distribution of FCN constructed from the distributions of the diatomic species CF($X^2\Pi_r$) and CN($X^2\Sigma^+$) by discarding the nonbonded charge distributions on C (as defined by the plane P_C) and joining the two fragments at the resulting planar surface through the C nucleus. The charge density contours (au) in this and all succeeding figures increase from the outermost one inward in the order $2, 4, 8 \times 10^n$ beginning with $n = -3$ to $n = +1$ in steps of unity.

or redistribution of charge within the system relative to the atoms and of the localized or delocalized nature of the distribution. They should also lead to a scheme for the classification of the bonding, thereby allowing for the relative or sequential comparisons upon which so much of chemical knowledge is organized and cataloged.

To meet these requirements and bearing in mind that there is no unique *a priori* method of partitioning a charge distribution between the nuclei in a molecule[3] we make the following requirements of any partitioning scheme.

(i) The partitioning procedure and all parameters characterizing the distribution are to be directly related to measurable (*i.e.*, calculable) properties of the molecular charge distribution itself, the only allowance for subjectivity then being relegated to the choice of what parameters are most useful.

(ii) The method should be applicable to any molecule in any state, ground or excited, neutral or charged.

(iii) The method should be independent of the analytical form of the wave function and of the method used in its derivation.

The Partitioning Procedure

The method of partitioning a charge distribution is illustrated in terms of the linear polyatomic molecule FCN, the charge distribution of which is illustrated in Figures 1a and 1b. In general, a molecular charge distribution is characterized by a peaking of the charge density in the regions of the nuclei, with these regions of high charge density being joined by bridges of charge density much lower in value. The peaks arise primarily from inner-shell or core densities, but there are substantial contributions from the valence density distribution as well. The bridging density is due almost entirely to the valence density distribution (except in those cases where the valence density has been almost completely transferred). The point at which the charge density reaches its minimum value along the internuclear axis between a pair of nuclei is sensitive to the extent to which charge is transferred and to the degree to which it is localized in the regions of the individual nuclei joined by the bridge of density. Thus, as Figure 1 illustrates, the form of the charge distribution itself suggests a "natural" partitioning of the total charge distribution in the form of planes (labeled as P_m and P_m' in Figure 1) perpendicular to the bond axis through the points on the bond axis at which the charge density attains its minimum values between pairs of adjacent nuclei. We define the number of electronic charges associated with the F nucleus in FCN, a number designated as t_F, as the integral of the total molecular charge distribution $\rho(r)$ from infinity on the left up to the plane P_m, an integration which may be formally represented by

$$t_F = \int_{\infty}^{P_m} \rho(r)\mathrm{d}r \qquad (1)$$

Integration of $\rho(r)$ from P_m to P_m' yields the total number of electronic charges associated with the C nucleus.

$$t_C = \int_{P_m}^{P_m'} \rho(r)\mathrm{d}r \qquad (2)$$

Similarly t_N is obtained by integration of $\rho(r)$ from P_m' to infinity on the right.[8]

The value of r along an internuclear axis at which $\rho(r)$ attains its minimum value between a pair of nuclei defines a set of bonded radii for the two adjoining populations. The bonded radius as defined by the minimum value of $\rho(r)$ will be labeled as r_A^B for a nucleus A bonded to nucleus B (see Figure 1). These radii reflect the particular bonding situation and they compare favorably with standard values for ionic or covalent radii in certain limiting situations. For example, the bonded radius for Li in LiF, r_{Li}^F, is found to be 1.13 au, identical with the value assigned to the Li^+ ion in Pauling's scale of ionic radii.

A study of almost 200 molecular charge distributions by the authors has shown that a set of charges resulting

(8) One could choose a surface of a more general shape than the plane P_m through the point of minimum density for the basis of the partitioning procedure. For example, one might consider a surface which cuts each contour line at its point of maximum curvature. The two definitions of the partitioning surface will yield identical results in the limit of equal nuclear charges ($Z_A = Z_B$), and in general will diverge seriously only for cases in which $Z_B - Z_A \gtrsim 3$, *i.e.*, in those cases where there is a considerable transfer of charge from A to B. However, even in such cases, *e.g.*, BeO, LiF, and BO^+ (Figures 1 and 2), the spatial volumes defined by the plane P_m and the more general surface differ significantly only in regions of low density, and hence the two choices do not yield radically different values for the total populations on the nuclei. Also, in linear molecules it might appear that charge density of symmetry other than σ symmetry plays no role in defining the point of minimum charge density on the internuclear axis and hence no role in the definition of P_m. This, is, however, not the case. Thus one finds considerable alteration in the σ charge density of an RHF molecular charge distribution upon excitation or ionization of an electron in a π orbital.[9] As the examples which follow illustrate, these changes are faithfully represented by changes in the position of the plane P_m.

(9) P. E. Cade, R. F. W. Bader, and J. Pelletier, *J. Chem. Phys.*, 54, 3517 (1971).

from a partitioning scheme (such as the t's defined above) is insufficient to characterize a molecular charge distribution. As important as the total charge t_A is its asymmetry with respect to a plane P_A perpendicular to the bond axis passing through the nucleus in question (Figure 1). When A is a terminal nucleus in a molecule the plane P_A divides t_A into a bonded and a nonbonded contribution

$$t_A = n_A + b_A$$

while if A is a centrally bonded nucleus $\cdots$BAC$\cdots$, the plane P_A will define two bonded populations

$$t_A = b_A{}^B + b_A{}^C$$

(where the bonded partner is indicated by a superscript). For the carbon atom in FCN, for example, the bonded populations $b_C{}^F$ and $b_C{}^N$ and their corresponding radii provide a measure of the asymmetry in the total population on carbon arising from its differential bonding with the fluorine and nitrogen.

The nonbonded charge for a terminal nucleus A in a molecule is obtained by integration of $\rho(r)$ from infinity on its nonbonded side up to the plane P_A. One finds that the spatial extension of the nonbonded charge density varies considerably depending upon the state of ionization or excitation. This is well illustrated in Figure 3 by the charge distributions of $BeF(X^2\Sigma^+)$ and $BeF^+(X^1\Sigma^+)$.[10] In BeF, the nonbonded charge density of the Be nucleus is diffuse and very extended in space, while in BeF^+ it is very compact, with values for the nonbonded charge and radius very close to those of a free Be^{2+} ion. Clearly, the nonbonded charge and its radius characterize the important properties of the region of a charge distribution dominated by the presence or absence of "unshared" or "lone pair" electrons.

The definition of a nonbonded radius requires the choice of a cutoff contour to define the "size" of a molecule. The 0.002-au contour is chosen as the outer contour in the display of $\rho(r)$ and in the determination of molecular sizes for the following reasons. (a) The region of space enveloped by this contour contains in general over 98% of the total electronic charge of the system.[11] (b) Lengths and widths as defined by this contour have been found to agree well with the few inferred experimental values for nonbonded molecular dimensions.[12] (c) The 0.002-au contour falls well out in the radial tail of the charge distribution where the density varies only slowly with further increases in distance from the molecular center. Thus the general shape of the distribution is well defined by this contour.

The radius of the nonbonded charge distribution is defined as the distance between a terminal nucleus and the 0.002-au contour on its nonbonded side as measured along the internuclear axis and is designated by the symbol $r_A{}^n$ for the nonbonded charge on nucleus A.

One further parameter is the value of $\rho(r)$ at the point of minimum density along the internuclear axis, labeled as $\rho(m)$. In molecular charge distributions characterized by extreme localization of the charge density in the regions of the individual nuclei with t_A, n_A, and $r_A{}^n$ values characteristic of the corresponding ions, $\rho(m)$ is very small in value. For example, in $LiF(X^1\Sigma^+)$ (Figure 2), $\rho(m) = 0.0802$ au, indicating that the charge distribution approaches that of two separate distributions of charge density in contact at their outer regions. In a system in which the valence charge density is more evenly delocalized over both nuclei, the value of $\rho(m)$ is considerably greater, *e.g.*, for $CN(X^2\Sigma^+)$, $\rho(m) = 0.4474$ au and for $N_2(X^1\Sigma_g^+)$, $\rho(m) = 0.7219$ au.

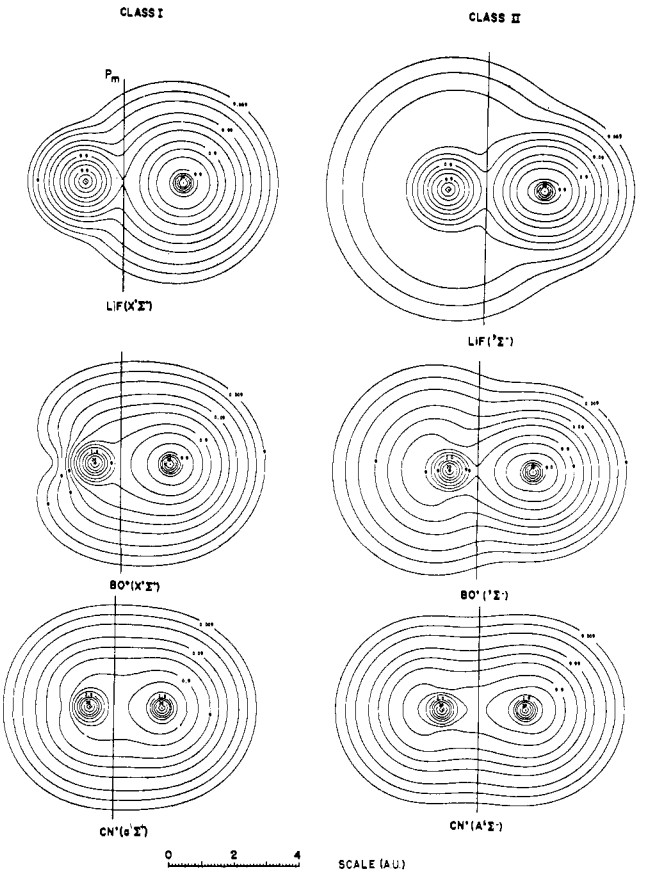

Figure 2. Molecular charge distributions typifying class I and class II systems. The partitioning planes P_m are indicated in this and succeeding figures.

The bulk of the present paper deals with the partitioning of the charge distributions of diatomic molecules. An interesting general question associated with any partitioning procedure is the extent to which the results are transferable between different systems. The diatomic results are an important first step in preparation for such intersystem comparisons at the charge density, rather than the orbital or geminal, level. The extent to which the populations as defined here are transferable between different systems is discussed and illustrated in this paper.

The integrations of $\rho(r)$ were performed using Gaussian quadrature methods. The boundary of the integrations was a cylinder capped by a hemisphere at each end such that any point on the boundary surface was 30 au from the internuclear axis. In each case, integration of $\rho(r)$ within the entire boundary surface yielded the correct total number of electrons to 1 part in 10^5, *i.e.*, to the stated accuracy of the coefficients defining the wave function.

(10) The prefix X before a state symbol signifies the ground state. For an explanation of the other labels, A, B, ..., a, b, ... see G. Herzberg, "Spectra of Diatomic Molecules," Van Nostrand, New York, N. Y., 1966, p 501.

(11) By actual integration of $\rho(r)$ within the 0.002-au contour one finds (electrons) 11.88 (or 99.00%) for LiF, 12.80 (or 98.46%) for CN, and 15.80 (or 98.75%) for NO^-.

(12) R. F. W. Bader, W. H. Henneker, and P. E. Cade, *J. Chem. Phys.*, 46, 3341 (1967).

Table I. $1\sigma^2 2\sigma^2 3\sigma^2 4\sigma^n 1\pi^m$

AB	Total charge populations t_A	t_B	Bonded and nonbonded charges b_A	n_A	b_B	n_B	ρ(m)	R	Bonded radius r_A^B	r_B^A	Nonbonded radius r_A^n	r_B^n
						$\ldots 4\sigma^2 1\pi^4$; $^1\Sigma^+$						
LiF X	2.16	9.84	1.11	1.05	4.99	4.85	0.0802	2.555	1.130	1.825	1.75	2.87
BeF^+ X	2.32	9.68	1.25	1.07	5.02	4.66	0.1601	2.572	0.917	1.655	1.42	2.75
BeO X	2.79	9.21	1.51	1.28	4.80	4.41	0.1842	2.515	0.894	1.621	1.39	3.11
BO^+ X	3.21	8.79	1.76	1.45	4.69	4.10	0.3032	2.275	0.767	1.508	1.28	2.90
CO^{2+}	3.78	8.22	2.06	1.72	4.52	3.70	0.4455	2.132	0.696	1.436	1.90	2.67
CN^+ a	4.56	7.44	2.29	2.27	4.15	3.29	0.3450	2.217	0.734	1.483	2.62	2.90
CC	6.00	6.00	3.14	2.86	3.14	2.86	0.2722	2.348	1.174	1.174	3.12	3.12
						$\ldots 4\sigma 1\pi^4$; $^2\Sigma^+$						
LiF^+ A	2.06	8.94	1.05	1.01	4.56	4.38	0.0539	2.955	1.212	1.743	1.69	2.54
LiO A	2.18	8.82	1.14	1.04	4.53	4.29	0.0475	3.184	1.256	1.928	1.72	2.90
BeO^+ A	2.45	8.55	1.34	1.11	4.58	3.97	0.1453	2.515	0.935	1.580	1.40	2.73
BeN A	3.19	7.81	1.41	1.78	4.22	3.59	0.0332	3.250	1.190	2.060	3.78	2.58
BN^+	3.40	7.60	1.86	1.54	4.31	3.29	0.2261	2.421	0.828	1.593	1.18	2.85
						$\ldots 1\pi^4$; $^1\Sigma^+$						
LiO^+ A	2.07	7.93	1.07	1.00	4.10	3.83	0.0249	3.184	1.373	1.811	1.68	2.27
						$\ldots 4\sigma^2 1\pi^3$; $^2\Pi_i$						
LiF^+ X	2.07	8.93	1.06	1.01	4.51	4.42	0.0745	2.955	1.145	1.810	1.70	2.78
LiO X	2.18	8.82	1.13	1.05	4.46	4.36	0.0673	3.184	1.185	1.999	1.74	3.21
BeO^+ X	2.43	8.57	1.33	1.10	4.43	4.14	0.1955	2.515	0.891	1.624	1.42	3.01
BeN	3.03	7.97	1.52	1.51	4.19	3.78	0.0758	3.250	1.100	2.150	2.98	3.12
BN^+ X	3.43	7.57	1.83	1.60	4.03	3.54	0.2602	2.421	0.806	1.615	2.22	3.08
CC^+	5.50	5.50	2.91	2.59	2.91	2.59	0.3076	2.348	1.174	1.174	2.95	2.95
						$\ldots 4\sigma^2 1\pi^2$; $^3\Sigma^-$						
LiO^+ X	2.08	7.92	1.06	1.02	4.00	3.92	0.0629	3.184	1.198	1.986	1.71	3.09
LiN	2.22	7.78	1.16	1.06	3.93	3.85	0.0603	3.400	1.224	2.176	1.76	3.35
BeC	3.31	6.69	1.55	1.76	3.52	3.17	0.0580	3.500	1.182	2.318	3.58	3.29
BB	5.00	5.00	2.55	2.45	2.55	2.45	0.1250	3.005	1.503	1.503	3.47	3.47
						$\ldots 4\sigma^2 1\pi$; $^2\Pi_r$						
LiC	2.30	6.70	1.21	1.09	3.38	3.32	0.0445	3.800	1.314	2.486	1.72	3.69
BeB	3.57	5.43	1.64	1.93	2.85	2.58	0.0409	4.000	1.385	2.615	3.75	3.50
BB^+	4.50	4.50	2.31	2.19	2.31	2.19	0.1484	3.005	1.503	1.503	3.27	3.27
						$\ldots 4\sigma^2$; $^1\Sigma^+$						
LiB	2.48	5.52	1.28	1.20	2.76	2.76	0.0269	4.500	1.466	3.034	1.72	4.06
BeBe	4.00	4.00	1.93	2.07	1.93	2.07	0.0476	4.000	2.000	2.000	3.92	3.92
						$\ldots 3\sigma^2$; $^1\Sigma^+$						
LiLi	3.00	3.00	1.68	1.32	1.68	1.32	0.0138	5.051	2.530	2.530	1.82	1.82

Characterization of Charge Distributions for Homonuclear and Heteronuclear Diatomic Molecules

Tables I–IV list the values of the parameters defined above for specific states for a number of homonuclear and heteronuclear diatomic molecules. The molecules are arranged in isoelectronic series (a given state of a given configuration), each series being ordered with respect to decreasing values of the difference in nuclear charges $|Z_A - Z_B|$.[13]

All molecules with states arising from certain general electronic configurations were found to have either similar values for the parameters characterizing their charge distribution or values which vary in a regular manner through given isoelectronic series. On this basis the states of the homonuclear and heteronuclear diatomic molecules are divided into four classes: class I, $1\sigma^2 2\sigma^2 3\sigma^2 4\sigma^2 1\pi^m$ and $1\sigma^2 2\sigma^2 3\sigma^2 4\sigma^n 1\pi^4$ (n = 0–2; m = 0–4) (Table I); class II, $1\sigma^2 2\sigma^2 3\sigma^2 4\sigma^2 5\sigma^2 1\pi^m$ and $1\sigma^2 2\sigma^2 3\sigma^2 4\sigma^2 1\pi^4 5\sigma^n$ (n = 1, 2; m = 4, 3, 2) (Table II); class III, $1\sigma^2 2\sigma^2 3\sigma^2 4\sigma^2 1\pi^4 2\pi^m$ (Table III); and class IV, $1\sigma^2 2\sigma^2 3\sigma^2 4\sigma^2 1\pi^4 5\sigma^2 2\pi^m$ (m = 1, 2, 3, 4) (Table IV).

(13) The diatomic wave functions employed here are all to or near to Hartree–Fock accuracy. Only a few of these wave functions have, however, been published (see ref 9 and 12 above for citations of the AH and A_2 systems which are described in the literature). An index of the quality of these results can be obtained from the total energy values which are summarized by M. Krauss in "Compendium of *ab initio* Calculations of Molecular Energies and Properties," NBS Technical Note No. 438, Dec 1967. In only a few cases are there even now lower energies available for these systems and states. Lower energies will probably come from approximations *beyond* the restricted Hartree–Fock approximation used throughout here. These wave functions were calculated at the University of Chicago on an IBM 7094-7040 system during 1964–1967 using computer programs constructed there by the Laboratory of Molecular Structure and Spectra under the leadership of C. C. J. Roothaan. These programs are briefly described by A. C. Wahl, *J. Chem. Phys.*, 41, 2600 (1964), and W. Huo, *ibid.*, 43, 624 (1965). The actual calculations for the systems reported here were carried out by a number of workers at LMSS including A. C. Wahl, W. Huo, J. Greenshields, G. Malli, and K. D. Sales, but most of the results involved here were the direct efforts and responsibility of one of the present authors (P. E. C.). A full documentation of these wave functions, a discussion of the flexibility of the basis sets, the extent and quality of orbital exponent optimization, etc., will be found in a publication in preparation by P. E. C. The authors are aware of no other *molecular* calculations on a scale and depth as that which forms the basis of this present work.

It should be realized that a number of the molecular species or states included in the tables correspond to systems which are experimentally unidentified. In some cases, on either experimental or theoretical grounds, there is no doubt that the system is physically stable though unobserved, *e.g.*, BF^+ or C_2^-, but in other cases we *may* be including the charge distribution of a system on a repulsive potential curve; *e.g.*, certainly this is true for the ground state of Be_2 and perhaps also for systems like NF^-, LiC, and LiN, etc.

Table II. $1\sigma^2 2\sigma^2 3\sigma^2 4\sigma^2 5\sigma^n 1\pi^m$

AB	Total charge populations t_A	t_B	Bonded and nonbonded charges b_A	n_A	b_B	n_B	ρ(m)	R	Bonded radius r_A^B	r_B^A	Nonbonded radius r_A^n	r_B^n
						$\ldots 5\sigma^2 1\pi^4$; $^1\Sigma^+$						
BeF^-	4.08	9.92	1.44	2.64	5.10	4.82	0.1499	2.572	0.930	1.642	4.68	2.85
BF X	4.26	9.74	1.56	2.70	5.09	4.65	0.2391	2.391	0.809	1.582	3.82	2.75
BO^-	4.70	9.30	1.76	2.94	4.87	4.43	0.3236	2.275	0.778	1.497	4.05	3.09
CF^+ X	4.52	9.48	1.77	2.75	5.03	4.45	0.3636	2.322	0.772	1.550	3.19	2.61
CO X	5.08	8.92	2.03	3.05	4.76	4.16	0.5101	2.132	0.723	1.409	3.42	2.93
CN^-	5.64	8.36	2.30	3.34	4.42	3.94	0.4878	2.214	0.767	1.447	3.61	3.31
NO^+ X	5.82	8.18	2.58	3.24	4.34	3.84	0.7608	2.007	0.783	1.224	2.93	2.75
NN X	7.00	7.00	3.43	3.57	3.43	3.57	0.7219	2.068	1.034	1.034	3.12	3.12
						$\ldots 5\sigma 1\pi^4$; $^2\Sigma^+$						
BeF X	3.24	9.76	1.32	1.92	5.02	4.74	0.1535	2.572	0.927	1.645	4.02	2.80
BeO^-	3.61	9.39	1.51	2.10	4.84	4.55	0.1877	2.515	0.899	1.616	4.34	3.18
BF^+ X	3.43	9.57	1.47	1.96	5.03	4.54	0.2527	2.391	0.807	1.584	3.30	2.68
BO X	3.93	9.07	1.73	2.20	4.78	4.29	0.3194	2.275	0.777	1.498	3.54	3.00
CO^+ X	4.40	8.60	2.04	2.36	4.64	3.96	0.5133	2.107	0.713	1.394	2.95	2.82
CN X	5.06	7.94	2.35	2.71	4.25	3.69	0.4474	2.214	0.763	1.451	3.17	3.16
NN^+	6.50	6.50	3.35	3.15	3.35	3.15	0.5731	2.113	1.057	1.057	2.81	2.81
CC^-	6.50	6.50	3.22	3.28	3.22	3.28	0.3633	2.348	1.174	1.174	3.49	3.49
						$\ldots 5\sigma^2 1\pi^3$; $^2\Pi_i$						
BeF A	3.86	9.14	1.44	2.42	4.71	4.43	0.1219	2.634	0.955	1.679	4.20	2.78
BeO^-	4.15	8.85	1.48	2.67	4.53	4.32	0.1905	2.515	0.902	1.613	4.69	3.15
BF^+ A	4.01	8.99	1.53	2.48	4.68	4.31	0.1433	2.640	0.868	1.772	3.50	2.70
BO A	4.32	8.68	1.60	2.72	4.52	4.16	0.2256	2.555	0.848	1.707	3.84	3.00
BN^-	4.78	8.22	1.81	2.97	4.27	3.95	0.3012	2.421	0.817	1.604	4.06	3.35
CO^+ A	4.68	8.32	1.86	2.82	4.39	3.93	0.4120	2.350	0.798	1.552	3.23	2.84
CN A	5.27	7.73	2.17	3.10	4.05	3.68	0.4567	2.330	0.828	1.502	3.44	3.18
NN^+	6.50	6.50	3.17	3.33	3.17	3.33	0.6188	2.222	1.111	1.111	2.93	2.93
CC^-	6.50	6.50	3.09	3.41	3.09	3.41	0.3517	2.588	1.294	1.294	3.64	3.64
						$\ldots 5\sigma^2 1\pi^2$; $^3\Sigma^-$						
LiF	3.53	8.47	1.58	1.95	4.38	4.09	0.0614	2.955	1.182	1.773	3.71	2.77
BeF^+ A	3.65	8.35	1.51	2.14	4.32	4.03	0.1197	2.572	0.943	1.629	3.53	2.67
BeO A	3.94	8.06	1.46	2.48	4.13	3.93	0.1844	2.515	0.904	1.661	4.25	3.04
BO^+	4.11	7.89	1.54	2.57	4.08	3.81	0.2088	2.555	0.844	1.711	3.58	2.90
BN	4.45	7.55	1.66	2.79	3.88	3.67	0.3142	2.421	0.817	1.604	3.89	3.23
CN^+ A	5.05	6.95	2.21	2.84	3.50	3.45	0.3734	2.576	1.102	1.474	3.27	3.07
CC A	6.00	6.00	2.84	3.16	2.84	3.16	0.3725	2.588	1.294	1.294	3.48	3.48
						$\ldots 5\sigma^2 1\pi^2$; $^1\Delta$						
LiF a	3.53	8.47	1.58	1.95	4.38	4.09	0.0610	2.955	1.183	1.772	3.71	2.76
BeF^+ a	3.65	8.35	1.52	2.13	4.32	4.03	0.1189	2.572	0.943	1.629	3.53	2.67
BeO a	3.94	8.06	1.46	2.48	4.13	3.93	0.1832	2.515	0.904	1.611	4.24	3.03
BO^+ a	4.12	7.88	1.55	2.57	4.08	3.80	0.2060	2.555	0.844	1.711	3.58	2.89
BN a	4.47	7.53	1.67	2.80	3.88	3.65	0.3113	2.421	0.816	1.605	3.88	3.23
CC	6.00	6.00	2.83	3.17	2.83	3.17	0.3732	2.588	1.294	1.294	3.48	3.48

Table III. $1\sigma^2 2\sigma^2 3\sigma^2 4\sigma^2 1\pi^4 2\pi^m$

AB	Total charge populations t_A	t_B	Bonded and nonbonded charges b_A	n_A	b_B	n_B	ρ(m)	R	Bonded radius r_A^B	r_B^A	Nonbonded radius r_A^n	r_B^n
						$\ldots 2\pi$; $^2\Pi_r$						
BeF H	3.12	9.88	1.46	1.66	5.10	4.78	0.1379	2.634	0.939	1.695	1.40	2.81
BF^+ H	3.35	9.65	1.67	1.68	5.07	4.58	0.2393	2.391	0.797	1.594	1.16	2.68
BO H	3.88	9.12	1.91	1.97	4.78	4.34	0.2831	2.275	0.770	1.505	1.72	2.99
CO^+ H	4.37	8.63	2.19	2.18	4.64	3.99	0.4265	2.107	0.692	1.415	2.10	2.77
CN H	5.12	7.88	2.40	2.72	4.26	3.62	0.3120	2.214	0.743	1.471	2.90	2.98

All molecules AB (*with* $Z_A < Z_B$) in states derived from the configurations in class I possess the following characteristics. (i) The bonded population exceeds the nonbonded population on both A and B ($b_A > n_A$ and $b_B > n_B$), and more than one-half of the total negative charge in these systems is found in the *bonded region*. (ii) The nonbonded charge and its radius on A vary from the corresponding free-ion values (see Table V) for A^+ or A^{2+} (*e.g.*, the $1s^2$ distributions in Li^+ and Be^{2+}) to values which in general are significantly less than the free-atom values, $n_A < {}^1/_2 Z_A$.[14] (iii) For the distribution of charge on B one finds $n_B > {}^1/_2 Z_B$ and nonbonded radii approximately equal to or slightly less than the negative ion values. For ionized states the values of n_B and r_B^n approach the corresponding values for the neutral atom B. (iv) There is a pronounced

(14) The only exceptions to any of the generalizations for any of the classes proposed here are BeC and BeB, the wave functions for which were calculated at the arbitrarily chosen internuclear separations of 3.50 and 4.00 au, respectively. In both these cases the nonbonded charge on Be is diffuse.

Table IV. $1\sigma^2 2\sigma^2 3\sigma^2 4\sigma^2 1\pi^4 5\sigma^2 2\pi^m$

AB	Total charge populations t_A	t_B	Bonded and nonbonded charges b_A	n_A	b_B	n_B	ρ(m)	R	Bonded radius r_A^B	r_B^A	Nonbonded radius r_A^n	r_B^n
						$\ldots 5\sigma^2 2\pi^4;\ ^1\Sigma^+$						
FF	9.00	9.00	4.41	4.59	4.41	4.59	0.2956	2.680	1.340	1.340	2.56	2.56
						$\ldots 5\sigma^2 2\pi^3;\ ^2\Pi_i$						
NF^- X	7.13	9.87	3.03	4.10	5.04	4.83	0.3029	2.489	0.933	1.556	3.03	2.75
FF^+	8.50	8.50	4.21	4.29	4.21	4.29	0.3753	2.525	1.263	1.263	2.52	2.52
						$\ldots 5\sigma^2 2\pi^2;\ ^3\Sigma^-$						
NF X	6.48	9.52	2.84	3.64	4.85	4.67	0.3420	2.489	1.021	1.468	2.98	2.66
NO^-	7.02	8.98	3.00	4.02	4.50	4.48	0.5755	2.175	0.887	1.288	3.14	2.98
OO	8.00	8.00	3.86	4.14	3.86	4.14	0.5513	2.282	1.141	1.141	2.83	2.83
FF^{+2}	8.00	8.00	4.02	3.98	4.02	3.98	0.3798	2.525	1.263	1.263	2.43	2.43
						$\ldots 5\sigma^2 2\pi^2;\ ^1\Delta$						
NF a	6.49	9.51	2.84	3.65	4.86	4.65	0.3484	2.472	1.006	1.465	2.98	2.66
OO a	8.00	8.00	3.86	4.14	3.86	4.14	0.5396	2.297	1.149	1.149	2.82	2.82
						$\ldots 5\sigma^2 2\pi^2;\ ^1\Sigma^+$						
NF b	6.50	9.50	2.84	3.66	4.86	4.64	0.3529	2.457	0.990	1.467	2.97	2.66
OO b	8.00	8.00	3.86	4.14	3.86	4.14	0.5246	2.318	1.159	1.159	2.82	2.82
						$\ldots 5\sigma^2 2\pi;\ \Pi^2_r$						
CF X	5.21	9.79	2.02	3.19	5.14	4.65	0.2924	2.402	0.778	1.624	3.35	2.70
NF^+ X	5.89	9.11	2.68	3.21	4.66	4.45	0.3765	2.489	1.106	1.383	2.89	2.56
NO X	6.50	8.50	2.90	3.60	4.34	4.16	0.5933	2.175	0.915	1.260	3.04	2.87
OO^+ X	7.50	7.50	3.69	3.81	3.69	3.81	0.7030	2.122	1.061	1.061	2.69	2.69
						$\ldots 5\sigma 2\pi;\ ^3\Pi$						
CO a	4.97	9.03	2.18	2.79	4.77	4.26	0.4016	2.285	0.761	1.524	3.02	2.92

Table V. Free-Atom and Ionic Radii (au)[a]

Atom	State	Radius of 0.002 contour	Atom	State	Radius of 0.002 contour
H	^2S	2.54	C^+	^2P	2.90
He	^1S	2.27	C^-	^4S	3.66
Li	^2S	3.29	N	^4S	3.06
Li	^2P	2.40	N	^2D	3.10
			N	^2P	3.13
Li^+	^1S	1.68			
			N^+	^3P	2.74
Be	^1S	3.67			
			N^-	^3P	3.53
Be^+	^2P	3.07			
Be^+	^2S	3.05	O	^3P	2.92
			O	^1D	2.94
Be^{2+}	^1S	1.35	O	^1S	2.97
B	^2P	3.50	O^+	^4S	2.59
			O^+	^2D	2.62
B^+	^3P	3.04			
B^+	^1S	3.04	O^-	^2P	3.34
B^{2+}	^2S	0.90	F	^2P	2.78
B^{3+}	^1S	1.14	F^+	^3P	2.49
			F^+	^1D	2.50
B^-	^3P	3.98			
			F^-	^1S	3.17
C	^3P	3.28			
C	^1D	3.31	Ne	^1S	2.65
C	^1S	3.36			

[a] Calculated from the wave functions of E. Clementi, "Table of Atomic Functions," Supplement to *IBM J. Res. Develop.*, 1965. Identical results are obtained using the "accurate basis sets" of P. S. Bagus and D. L. Gilbert, reported in R. F. W. Bader and P. M. Beddall, *Chem. Phys. Lett.*, **8**, 29 (1971).

charge transfer from A to B with $t_A < Z_A$ and $t_B > Z_B$, or in certain ionized states $t_B \sim Z_B$. (v) In the homonuclear limit the charge distribution assumes the characteristics of that on an A nucleus; $b_A > n_A$, and r_A^n and n_A less than the corresponding atomic values.

Charge distributions of class I systems are exemplified (Figure 2) by the $^1\Sigma^+$ states of LiF, BO^+, and CN^+ and by the $^1\Sigma^+$ state of BeF^+ (Figure 3). The charge distributions shown in Figure 2 for the $^1\Sigma^+$ states illustrate the change in n_A and r_A^n from values almost identical with the free-ion core (Li^+ in LiF) to limiting values less than those of the free atom (C in CN^+) as $Z_A \rightarrow Z_B$. The pinched effect of the contours in the nonbonded region of boron in the intermediate case of BO^+ are characteristic of a considerable A → B charge transfer in the σ system with a diffuse back-transfer (B → A) in the π system. This effect is common for class I systems for which Z_B exceeds Z_A by two or three units and, in extreme cases such as BO^+, is characterized by an r_A^n value approximately equal to that of the $1s^2$ core density but an n_A value in excess of unity.

It is primarily the nature of the charge distribution on A ($Z_A < Z_B$) which distinguishes class II and III systems from those of class I. This is dramatically illustrated in Figure 2, which contrasts the charge distributions of the $^1\Sigma^+$ states (class I) with those of the $^3\Sigma^-$ states (class II) for LiF, BO^+, and CN^+. Class II systems possess a relatively large nonbonded charge population on A, the distribution of which becomes increasingly diffuse as $|Z_A - Z_B|$ increases. This behavior of the nonbonded charge on A is just the opposite of that found for class I systems. The primary characteristics of class II systems (systems with single or double occupation of the 5σ orbital) are as follows. (i) The nonbonded charge on A *exceeds* its bonded charge, $n_A > b_A$. While b_B is still greater than n_B in these systems, more than one-half of the total electronic charge is now distributed in the nonbonded regions of A and B. For example, CN^+ in its $^3\Sigma^-$ state (class II) has an excess of 0.58 e in the *nonbonded* regions while its $^1\Sigma^+$ state (class I) has an excess of 0.88 e in the

bonded region. (ii) When the 5σ orbital is doubly occupied, $n_A > {}^1/_2 Z_A$ and $r_A{}^n$ exceeds that of the free atom. (iii) The value of the nonbonded charge and its radius on B approach those for neutral B (or B^+ in the ionized states). (iv) There is a general reduction in the extent of charge transfer from A to B for a given molecule on passing from a class I to a class II state, as reflected in the values of n_B and $r_B{}^n$ decreasing from values near those for B^- or B in class I to values near those for B or B^+ in class II. For example, t_C in CN^+ increases from 4.56 to 5.05 on excitation from its $^1\Sigma^+$ to its $^3\Sigma^-$ state. (v) In the homonuclear limit the charge distributions again exhibit the characteristics of the A distribution for the class in question ($3\sigma_g$ being the limiting form of the 5σ orbital). Thus N_2, for example, exhibits a *nonbonded* charge excess of 0.28 e. The C_2 molecule has a *nonbonded* charge excess of 0.64 e in its $^3\Sigma_g^-$ state (class II), but a *bonded* charge excess of 0.56 e in its $X^1\Sigma_g^+$ state (class I).

Systems in class III possess the same distinguishing characteristics as those of class II with the exception that the charge distribution on A is *increased in width perpendicular* to the bond axis, as opposed to the axial extension found in class II. As in class II, the distribution of the nonbonded charge in A for states in class III becomes increasingly diffuse as $|Z_A - Z_B|$ increases. A comparison of the parameters for the $H^2\Pi_r$ states in Table III with those for the $\ldots 1\pi^4 5\sigma$; $^2\Sigma^+$ states of the corresponding systems in Table II shows the values of t_A and t_B to be identical, to the nearest tenth of a charge, and the distribution of the charge on B to be similar in the two classes.

The nonbonded charge on A is in general about 0.5 e larger for states in class III than for those in class I. Since this increase in n_A is confined primarily to a π distribution on A, the "pinch effect" referred to earlier for intermediate members of class I is very pronounced in class III. This effect is exhibited by all of the members of class III to a diminishing extent as $Z_A \rightarrow Z_B$ and is most extreme in the first member $BeF(H^2\Pi_r)$, Figure 3. The radius of the nonbonded charge on Be in the $H^2\Pi_r$ state (as measured along the molecular axis) is identical with that found in the $X^1\Sigma^+$ state of BeF^+, but the amount of nonbonded charge in the $H^2\Pi_r$ state exceeds that in the $X^1\Sigma^+$ state by 0.59 e.

The distinguishing features of the charge distribution for classifications I, II, and III are illustrated in Figure 3 for three states of the BeF system. A comparison of these distributions illustrates the very marked change in the characteristics of $\rho(r)$ entailed by the occupancy or lack of occupancy of the 2π or 5σ orbitals. The other three states of the BeF system listed in the tables [BeF^+-($^3\Sigma^-$), $BeF(A^2\Pi_i)$, $BeF^-(^1\Sigma^+)$] all involve double occupancy of the 5σ orbital and the charge distributions of all three exhibit the same characteristics as those for the $^2\Sigma^+$ ground state.

Class IV systems are characterized, as are systems in classes II and III, by $n_A > b_A$, $n_B < b_B$, and $(n_A + n_B) > (b_A + b_B)$. However, in class IV systems the nonbonded radii on both A and B are approximately equal to or *less* than the atomic values. Thus simultaneous occupation of the 5σ and 2π orbitals (to give class IV states) leads to a contraction of the nonbonded charge distributions on A and B compared to systems with either the 5σ *or* 2π orbital occupied.

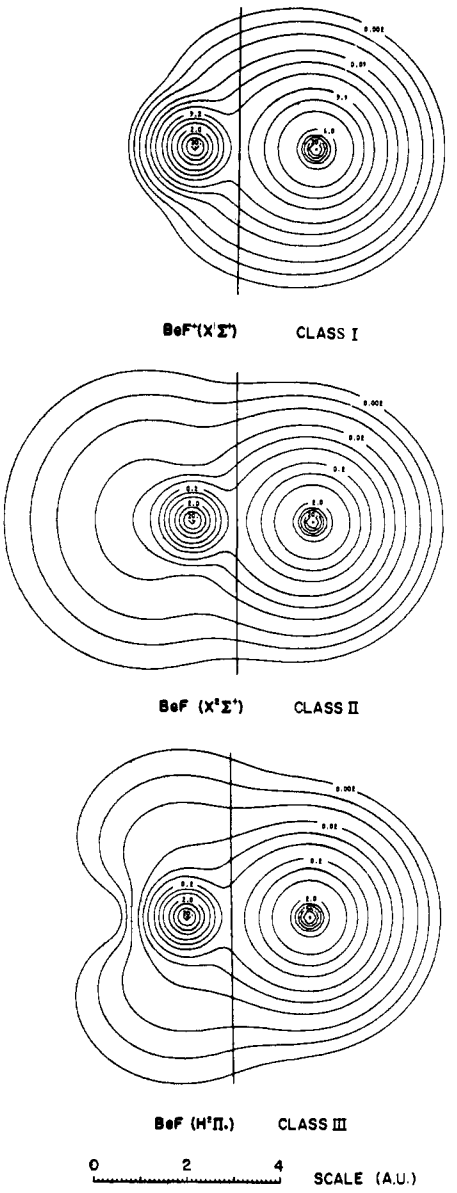

Figure 3. Molecular charge distributions for the BeF system illustrating the distinguishing features of classes I, II, and III.

The neutral species with these configurations exhibit a charge transfer A → B in the range from 0.5 to 1 e. This classification is typified by the charge distribution for the $a^3\Pi$ state of CO shown in Figure 4, where all four classification schemes are illustrated for the CO system. Note the increase in the radius of the nonbonded charge on carbon from values less than the atomic value in CO^{+2} (class I) and CO^+ (class III) to a value greater than the atomic value in the $X^1\Sigma^+$ ground-state distribution (class II) and its final decrease to less than the atomic value in the $a^3\Pi$ excited state (class IV). Two other states of CO^+ both from classification II are also illustrated in Figure 4 ($\ldots 5\sigma 1\pi^4$; $X^2\Sigma^+$ and $\ldots 5\sigma^2 1\pi^3$; $A^2\Pi_i$) to illustrate that the classification is determined more by the electronic state of the system rather than by its state of ionization. Thus the $H^2\Pi_r$ state of CO^+ in which the 5σ orbital is vacant possesses smaller values for n_C and $r_C{}^n$ than do the states with single and double occupation of this orbital.

While the numbers listed in the Tables I–IV are independent of the molecular orbital nature of the wave

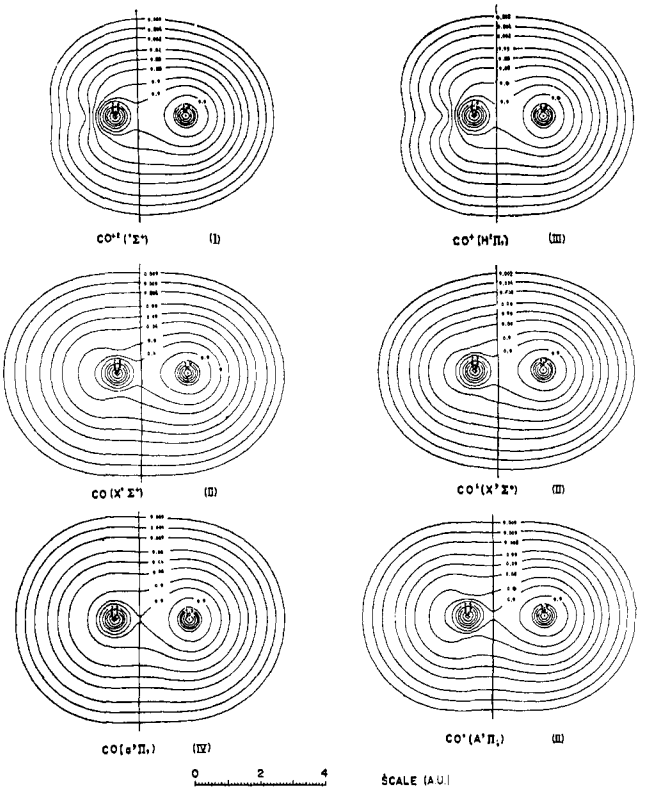

Figure 4. Molecular charge distributions for the CO system for states from class I to IV.

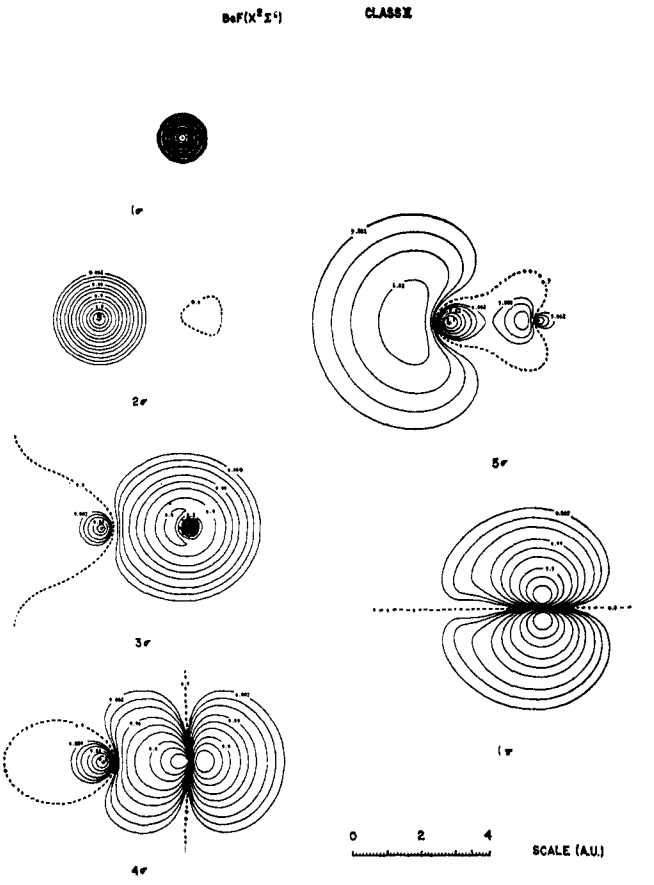

Figure 5. Molecular orbital charge density distributions for BeF-($X^2\Sigma^+$).

function, the Hartree–Fock molecular orbitals obviously provide a very suitable framework for the prediction and understanding of the gross features of a molecular charge distribution. Each orbital density distribution has certain distinguishing spatial characteristics and limiting forms. Thus we preface the discussion of various trends exhibited by the values of the parameters listed in the tables with a brief examination of the general features of the Hartree–Fock molecular orbitals for heteronuclear diatomic systems of first-row atoms (Li to F).

Figures 5 and 6 illustrate the molecular orbital charge distributions for BeF($X^2\Sigma^+$) and CO($a^3\Pi$), respectively. These cases are chosen since they illustrate the principal changes in the orbital densities when the atoms forming the molecule are from widely separated ($Z_B - Z_A$ = 3–6) or near or neighboring families of the periodic table ($Z_B - Z_A$ = 1, 2).[15]

The 1σ and 2σ charge densities are in every case slightly polarized 1s atomic-like distributions localized on the B and A nuclei, respectively. The 3σ and 4σ charge densities are heavily localized on the B nucleus and approach respectively the limiting forms of polarized 2s and $2p\sigma$ atomic-like distributions on B when A ≡ Li, Be, or B and B ≡ F, O, or N. The 3σ density becomes only slightly less delocalized as the nuclear charges of A and B approach one another (short, of course, of $Z_A = Z_B$). The 4σ density does become increasingly delocalized over both nuclei as Z_A approaches Z_B in value. The density in the region of the A nucleus is, however, much more diffuse and lower in absolute amount than that accumulated in the nonbonded region of the B nucleus.

(15) The forms of the molecular orbitals for the homonuclear limit ($Z_A = Z_B$) are given by A. C. Wahl, *Science*, **151**, 961 (1966).

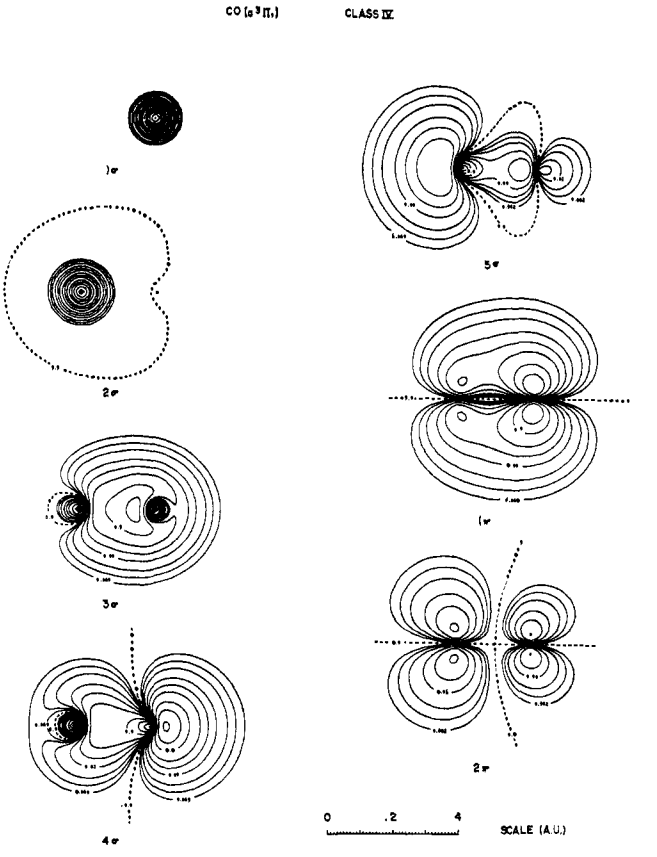

Figure 6. Molecular orbital charge density distributions for CO-($a^3\Pi_r$).

The 5σ density is largely confined to a diffuse distribution of considerable spatial extent on the nonbonded side of the A nucleus when $Z_B - Z_A = 3$–5. As Z_A approaches Z_B in value the 5σ density is delocalized over both nuclei, concentrated in the nonbonded regions of both A and B, with the nonbonded distribution of A being more diffuse and of larger spatial extent than that on B.

The 1π density is largely localized on the B nucleus, a localization that decreases as Z_A approaches Z_B in value. It is a slight delocalization of the 1π density which is primarily responsible for the nonbonded charges on Be and B in states from Table I exceeding the value of unity characteristic of a $1s^2$ core contribution. The pinch effect in the nonbonded charge distributions on A in states from Table I has its origin in this same delocalization of the 1π density and is indicative of a change from nonbonding to a slightly bonding role for this orbital as $Z_A \rightarrow Z_B$. The characteristics of the density distribution of the 2π orbital are similar to those found for the 5σ orbital. When $Z_B - Z_A = 5$, 4, or 3, the 2π density is largely localized on A in the form of a diffuse distribution polarized into the nonbonded region of A. These characteristics of the 2π density are very evident in the distribution of nonbonded charge density on Be in the $H^2\Pi_r$ state of BeF (Figure 3). As the difference in the nuclear charges on A and B decreases, the 2π density becomes less diffuse and more equally partitioned between distributions separately localized on A and B, but with the distribution on A exceeding in amount and spatial extent that on B. Thus occupation of the 5σ orbital results in an axial expansion of the nonbonded charge distribution on A, while occupation of the 2π orbital increases its radial extension perpendicular to the bond axis.

In molecules (with as usual $Z_A < Z_B$) in which the 5σ orbital is vacant, *e.g.*, ground states of LiF, BeF^+, and LiO, the valence density will be localized in the region of the B nucleus. Single or double occupation of the 5σ orbital will lead to a marked extension of the valence charge density into the nonbonded region of the A nucleus. Thus in molecules such as BeF ($\ldots 5\sigma^1$) or BF ($\ldots 5\sigma^2$) the $3\sigma^2$, $4\sigma^2$, and $1\pi^4$ charge distributions are still largely localized on F, but the overall charge distribution will appear rather symmetrical and tend to exhibit a large dipole moment $A^{\delta-}B^{\delta+}$ because of the extreme localization of the 5σ charge density in the nonbonded region of the A nucleus.

Periodic Variations in the Populations t_A

Figure 7 illustrates the variation in the electronic charge populations associated with the nuclei Li to F when in combination with other first-row members of the periodic table. All values refer to the ground-state (where known and otherwise assumed) charge distributions.

The value of t_{Li} shows a monotonic decrease for the diatomic combinations of Li across the first period of the table. A large transfer of charge occurs early in the Li series; t_{Li} in LiB already indicates a transfer of 0.52 e to B, and reaches a limiting value of 0.84 e to F in LiF. Oxygen and nitrogen are nearly as effective as fluorine in stripping charge density from Li, the net increases in t_O and t_N relative to the atomic values being 0.82 e and 0.78 e, respectively. The nonbonded charge on Li in its

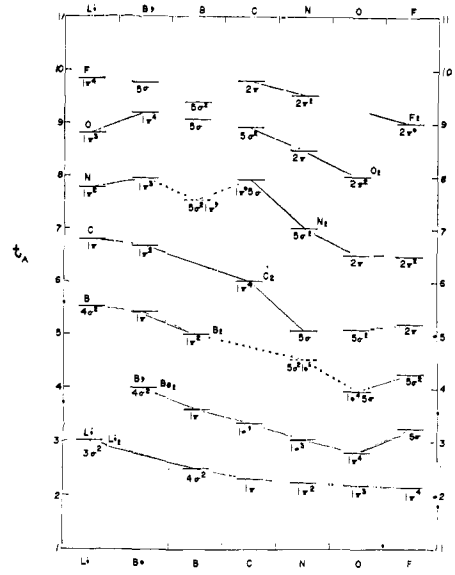

Figure 7. Variations in the total population t_A in diatomic species AB for A and B = Li → F.

nitride, oxide, and fluoride is close to unity, indicating an almost total loss of the valence charge density from the nonbonded region of Li in these compounds.

The transfer of charge density from Be to its bonded partner also increases in extent across the table but reaches a maximum value in BeO, corresponding to a transfer of 1.21 e from Be to O. The formation of BeF involves the occupation of the 5σ orbital, the density of which is heavily localized in the nonbonded region of Be. Thus one of the valence electrons partially transferred to O in BeO is almost totally localized in the nonbonded region of Be in BeF ($n_{Be} = 1.92$), and consequently the extent of charge transfer from Be to O is greater than from Be to F. This fact is a reflection (as are the molecular orbital descriptions) of the simple valency notion that oxygen has two orbital vacancies compared to fluorine's one. The remarkable feature of the charge distribution of BeF (or BF) is the extent to which the nonbonded valence density is localized in the nonbonded region of Be (or B). In fact, the *valence* contributions to the nonbonded density on Be and B in their fluorides (0.9 and 1.7 e, respectively) indicate that 90 and 85% of the nonshared valence charge are localized in the nonbonded regions of the Be and B nuclei, respectively. This observation is rationalized on the basis of a strong repulsion of the relatively loosely bound nonbonded density by the large excess of negative charge localized on the F.

No wave function is available for $BC(^2\Pi_i)$ or for the $^3\Pi$ ground state of BN which has the configuration $\ldots 1\pi^3 5\sigma$.[16] The values of t_B and t_N indicated by the dashed levels in Figure 7 for BN are for the $^3\Sigma^-$ state derived from the configuration $\ldots 5\sigma^2 1\pi^2$. The molecule BO falls in the regular sequence with a configuration $\ldots 5\sigma^1 1\pi^4$. The transfer of 1.07 e from B to O is less than the 1.21 e found in BeO. Because of the single orbital vacancy in F compared to the double one in O, or equivalently stated, because of the double occupancy of the 5σ orbital in BF compared to its single occupancy in BO, the charge transfer from B is greater in its oxide than in its fluoride. Correspondingly the nonbonded

(16) K. Douglas and C. Moser, *J. Chem. Phys.*, 46, 35 (1967).

charge on B increases from 2.20 e in its oxide to 2.70 e in its fluoride.

The variations in the values of the remaining populations, $t_C - t_F$, may be similarly interpreted in terms of the change in orbital configuration and class of the system. Thus t_F exhibits two minima, the first at BF, corresponding to the filling of the 5σ orbital (class II), and the second at F_2, corresponding to the filling of the $2\pi(1\pi_g)$ orbital (class IV).

Ionization and Excitation

Cade, Bader, and Pelletier[9] have presented a detailed discussion of the effects of excitation, ionization, and electron attachment on a diatomic molecular charge distribution. In this section the parameters proposed here are shown to summarize the important changes in the charge distribution brought about by these processes.

The first important observation is that states arising from the same electronic configuration have almost identical charge distributions (at least in RHF approximation). Thus parameters characterizing the $^3\Sigma^-$ state derived from the configuration $\ldots 5\sigma^2 1\pi^2$ (Table II) are almost identical for a given system with those for the corresponding $^1\Delta$ state derived from the same configuration. The $^3\Sigma^-$, $^1\Delta$, and $^1\Sigma^+$ states of NF and O_2 derived from the configuration $\ldots 5\sigma^2 2\pi^2$ and $\ldots 3\sigma_g^2 1\pi_g^2$ again illustrate the insensitivity of $\rho(r)$ to changes in Λ or the spin multiplicity (for the same configuration). (Some of the parameters for the states of NF and O_2 do differ slightly as the calculations are reported for each state at its own equilibrium value of R.) The fact that the three equilibrium values of R in these cases are so nearly the same is an experimental verification of the near identity of their charge distributions. Near identical charge distributions imply identical forces exerted on the nuclei and hence near identical values for R_e for the attainment of electrostatic equilibrium.[9]

Tables I and II provide two examples of excitation in which *no* new orbitals are involved, but a shift in occupation numbers occurs: in Table I the excitation ($\ldots 4\sigma^2 1\pi^3, X^2\Pi_i \rightarrow \ldots 4\sigma 1\pi^4, A^2\Sigma^+$) involving a $4\sigma \rightarrow 1\pi$ jump and in Table II the excitation ($\ldots 4\sigma^2 5\sigma 1\pi^4$, $X^2\Sigma^+ \rightarrow \ldots 4\sigma^2 5\sigma^2 1\pi^3, A^2\Pi_i$) with a $1\pi \rightarrow 5\sigma$ jump. Note that in both cases there is no change in the group classification upon the excitation. In the first excitation (LiF^+, LiO, BeO^+, BeN, BN^+) there is almost no change at all as $4\sigma \rightarrow 1\pi$ in t_A and t_B (or n_A or n_B). The pronounced localization of both 4σ *and* 1π density on the B nucleus is thus evident. In case of the second excitation (BeF, BF^+, BO, CO^+, CN, N_2^+, *e.g.*) there is substantial charge transfer B → A with the $1\pi \rightarrow 5\sigma$ jump as one would expect since 1π is localized mostly on the B nucleus and 5σ is concentrated (especially for large $|Z_A - Z_B|$) in the nonbonded region of A.

Finally there are very pronounced changes in $\rho(r)$ for excitations in which a new orbital is occupied, *e.g.*, in the excitation ($\ldots 4\sigma^2 1\pi^4$, $X^1\Sigma^+ \rightarrow \ldots 4\sigma^2 5\sigma^2 1\pi^2, {}^3\Sigma^-$ or $^1\Delta$), where $1\pi^2 \rightarrow 5\sigma^2$. The excitation causes a considerable transfer of charge from B back to A, ranging from 1.37 e in LiF to 0.49 e in CN^+. More striking still is the large increase in the overall length of the distributions as evidenced by the considerable increase in the nonbonded radius of A. These are the expected consequences of a maximal change in the occupation of the 5σ orbital.

In the ionization of LiF and LiO nine-tenths of the charge lost on ionization is removed from the regions of the fluorine and the oxygen (*i.e.*, from t_F and t_O). Only one-tenth of a charge is lost by the Li in both cases, and the nonbonded charge on Li remains essentially constant. These small changes in t_{Li} on ionization indicate that the charge populations on the Li nucleus in LiF and LiO are largely the tightly bound $1s^2$ core density. The values of t_{Li} in the neutral species and their change on passing to the ion indicate that an amount of valence charge in slight excess of 0.1 e is present on the Li in LiF and LiO. The populations on the lithium nucleus clearly approach the limiting form of a pure core density more closely in the ions LiF^+ and LiO^+ than they do in the neutral molecules.

The ionization of LiO may be contrasted with the ionization of BeO. In BeO only 0.64 charge is removed from the oxygen on ionization, the remaining 0.36 charge being lost by the Be. These figures are in part a reflection of the transfer of 1π density from B to A which is negligible in lithium compounds but becomes increasingly important for beryllium, boron, and carbon.

The containment of the charge loss on ionization to the region of the nucleus with the smallest nuclear charge is observed in the loss of the single unpaired 5σ electron from the $^2\Sigma^+$ states with the configuration $\ldots 5\sigma 1\pi^4$ to give the closed-shell "tight" $^1\Sigma^+$ distributions of the configuration $\ldots 1\pi^4$. The charge population on Be decreases by 0.92 e upon ionization of BeF, 0.85 of the charges being removed from the nonbonded region of Be. The localization of the charge removal decreases through the molecules listed in the $^2\Sigma^+$ series, corresponding to the more even distribution of the 5σ density which occurs as Z_A approaches Z_B in value. In the ionization of CN, 0.5 e is lost by both carbon and nitrogen.

Partitioning Molecular Properties. The Dipole Moment

The partitioning procedure proposed here divides the charge distribution into specific spatial contributions, each of which may be associated with a particular nucleus in the molecule. Thus any molecular property determined by the charge distribution may itself be partitioned by the same scheme into a corresponding set of separate contributions. The principal reason for such a partitioning of molecular properties is presumably to define additive, or nearly additive contributions to the property from the separate density contributions. Thus if $\rho_A(r)$ denotes the charge density assigned to a terminal nucleus A in A–B$\cdots$ by the partitioning procedure, then to what extent are the contributions to a given property constant or additive (from either the total or just the bonded density on A, $\rho_A^B(r)$) as the neighbor B occurs in different chemical environments? Usually one parcels out a given molecular property among "atoms" by means of a breakdown of localized molecular orbitals or LCAO coefficients, but the partitioning as proposed here accomplishes these objectives directly.

The electric dipole moment may be taken as an example, with some interesting physical aspects as well. The electric dipole moment for a diatomic molecule AB

with N electrons is

$$\mu = -\alpha RZ_A - \int_A z\rho(r)dr + (1 - \alpha)RZ_B - \int_B z\rho(r)dr \quad (3)$$

The coordinate system origin is located αR to the right of nucleus A along the internuclear axis; R is the internuclear separation. The integration over electronic coordinates is schematically indicated over "A" and "B" spatial regions. If we now identify αR as the intercept of the plane P_m on the internuclear axis and evaluate the integrals with respect to coordinate systems on nuclei A and B

$$\mu = -\alpha R(Z_A - t_A) - \int z_A\rho_A(r)dr_A + (1 - \alpha)R(Z_B - t_B) - \int z_B\rho_B(r)dr_B \quad (4)$$

where, for example

$$\int_A \rho(r)dr = \int \rho_A(r)dr_A = t_A \quad (5)$$

Equation 4 can be written as (using in addition $t_A + t_B = N$)

$$\mu = -\alpha R(Z_A + Z_B - N) + R(Z_B - t_B) + \mu_A + \mu_B \quad (6)$$

where

$$\mu_A = -\int z_A\rho_A(r)dr_A \text{ and } \mu_B = -\int z_B\rho_B(r)dr_B$$

These latter two quantities are simply the dipole moments of the charge densities associated with nuclei A and B in the molecule. For a neutral AB system

$$\mu = (Z_B - t_B)R + \mu_A + \mu_B \quad (7)$$

or, defining the charge-transfer contribution to the dipole moment to be μ_{CT}

$$\mu = \mu_{CT} + \mu_A + \mu_B$$

Thus in a molecule composed of nearly spherical distributions so that $\mu_A = 0$ and $\mu_B = 0$, the dipole moment is equal to the net charge transfer times the internuclear separation, μ_{CT}. Using the dipole moment to calculate a point-charge model of the distribution will yield a very unrealistic result if the charge distribution is not well approximated by spherical nonpolarized charge distributions on each nucleus. The only neutral molecules with charge distributions approaching these ideal (and unattainable) conditions are the compact distributions of class I with states derived from the configurations $\ldots 4\sigma^n 1\pi^m$.

Table VI lists the calculated dipole moments and the three contributions μ_{CT}, μ_A, and μ_B for a number of systems from all four classes. As anticipated the point charge model of μ ($\mu \sim \mu_{CT}$) is a reasonable one for inferring the extent of charge transfer for systems in class I.

The dipole moment of any state derived from a configuration with a nonzero occupation number for the 5σ orbital will not yield any meaningful measure of the extent of charge transfer when employed in a point-charge model analysis. The extreme asymmetry of the charge distribution on A together with its diffuse extension into the nonbonded region caused by the occupation of the 5σ orbital contribute a heavy weighting to the dipole moment operator, a weighting far out of proportion to the amount of charge on A in a point-charge model. Thus the values of μ_A are all large in magnitude and negative in sign for systems in class II, and in general $\mu < \mu_{CT}$ and in some cases is reversed in sign. For all the systems in classes II, III, and IV the contributions μ_A and μ_B oppose the charge-transfer contribution to μ (a reflection of the fact that for these classes $n_A > b_A$ and $b_B > n_B$) and in addition $|\mu_A| > |\mu_B|$. This latter inequality is most pronounced in class II systems, as expected. The variations in μ evident in Table VI reflect the detailed discussions already given for the variations in the charge distributions between and within classes. Thus the excitation BeO ($X^1\Sigma^+$, class I, $\ldots 1\pi^4$) → BeO ($^3\Sigma^-$, class II, $\ldots 1\pi^2 5\sigma^2$) results in a sign change and large increase in the magnitude of $|\mu_A|$. The excitation CN($X^2\Sigma^+$) → CN($A^2\Pi_i$) corresponding to the configuration change $\ldots 5\sigma 1\pi^4 \rightarrow \ldots 5\sigma^2 1\pi^3$ increases the magnitude of $|\mu_A|$ and hence reduces the value of μ itself. Excitation of a 5σ electron to a 2π orbital, BeF($X^2\Sigma^+$) → BeF($H^2\Pi_r$), reduces $|\mu_A|$ and in general increases μ.

Table VI. Partitioning of Dipole Moment[a] in AB Molecules

AB	State	μ_{CT}	μ_A	μ_B	μ
		Class I			
LiF	$X^1\Sigma^+$	6.34	0.14	−0.19	6.29
BeO	$X^1\Sigma^+$	7.76	0.20	−0.52	7.44
LiO	$X^2\Pi_i$	6.67	0.19	−0.05	6.81
BeN	$^2\Pi_i$	8.05	−0.84	−1.46	5.74
		Class II			
BF	$X^1\Sigma^+$	4.47	−4.46	−0.95	−0.94
CO	$X^1\Sigma^+$	5.00	−3.72	−1.01	0.27
BeF	$X^2\Sigma^+$	4.99	−3.32	−0.52	1.15
CN	$X^2\Sigma^+$	5.31	−2.04	−0.82	2.45
CN	$A^2\Pi_i$	4.32	−3.56	−0.47	0.29
BeO	$^3\Sigma^-$	0.39	−5.26	−0.10	−4.97
		Class III			
BeF	$H^2\Pi_r$	5.87	−1.12	−0.74	4.01
CN	$H^2\Pi_r$	4.93	−1.70	−1.15	2.08
		Class IV			
CF	$X^2\Pi_r$	4.83	−3.77	−1.36	−0.29
NO	$X^2\Pi_r$	2.75	−2.52	0.10	0.33

[a] All values are in debyes. A positive value implies the direction A^+B^- for μ.

Partitioning in Linear Polyatomics. Transferability

The result of partitioning the charge density in linear polyatomic systems is illustrated in Figure 8 for the molecules FCN, CO_2, and N_2O.[17] The population numbers listed above the internuclear axis are determined by the charge distribution of the polyatomic molecule. The transferability of the nonbonded, bonded, and total populations between different systems (in this case from diatomic to triatomic) may be judged from a comparison of these populations with the corresponding values listed below the molecular axis. These latter values are taken from the related diatomic fragments as listed in Tables II and IV. The estimated total population for a centrally bonded nu-

(17) The wave functions for the linear polyatomic systems are from the tabulation by A. D. McLean and M. Yoshimine, "Tables of Linear Molecule Wave Functions," Supplement to *IBM J. Res. Develop.*, Nov 1967. The most accurate of the tabulated sets were used for each system.

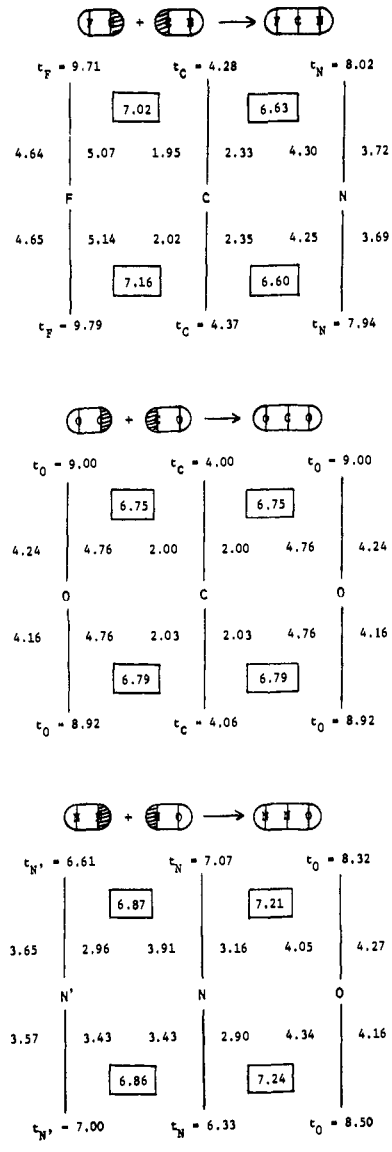

Figure 8. Comparison of the populations as defined by the planes P_m and P_A between triatomic systems (upper values) and diatomic fragments (lower values) for FCN, CO_2, and NNO.

cleus is equated to the two *bonded* populations of the relevant diatomic species. For example, in FCN, $t_C = b_C^F + b_C^N$, with b_C^F from $CF(X^2\Pi_r)$ and b_C^N from $CN(X^2\Sigma^+)$.

The FCN and CO_2 systems provide examples in which the total populations and the individual contributions to the total populations are transferable from the diatomic fragments to the polyatomic systems to within ~0.1 e. The largest error in an estimated total population occurs for C in FCN, where the sum of b_C^F and b_C^N overestimates the population on carbon by 0.09 e. The *total bonded* populations (the boxed values in Figure 8) and their individual contributions characterizing the C–N ($b_C^N + b_N^C$) and C–O ($b_O^C + b_C^O$) bonds are almost unchanged from the corresponding diatomic values. The bonded population of the F–C bond, ($b_F^C + b_C^F$) decreases by 0.14 e from the diatomic case. While the bond lengths in the polyatomic systems are different from those in the corresponding diatomic fragments, the ratio of the bonded radii for a bonded pair remains almost unchanged, indicating that the *relative* position of the partitioning plane P_m remains unchanged as the bond length is increased or decreased on passing from the diatomic to the polyatomic system. These ratios are (listing the diatomic value first in each case): $r_F^C/r_C^F = 2.09, 2.06$; $r_C^N/r_N^C = 0.53, 0.52$; and $r_O^C/r_C^O = 1.95, 1.96$.

The molecule NNO provides an example of a case in which the individual bonded and total populations change, but the nonbonded and *total bonded* populations remain almost constant. The estimated total populations on the terminal nitrogen (N′) and oxygen are too large; that on the central nitrogen is too small. There is an obvious transfer of charge from N′ and O to the central nitrogen when N_2O is compared to N_2 and NO. However, the *total bonded* populations for the N′–N and N–O bonds remain essentially unchanged between the triatomic and diatomic situations. Thus the increase in charge density on the central N is a result of a transfer of *bonded* charge from N′ to the $b_N^{N'}$ bonded population and from the bonded charge on oxygen to b_N^O. There is a redistribution of charge within the two bonded regions, but no significant transfer across the plane through the central N nucleus P_N.

Thus when there is a considerable change in the charge distribution of a fragment due to a change in its bonding environment, the change appears to be primarily restricted to a redistribution of charge within the bonded region. This is further illustrated by a comparison of the populations of the substituted acetylenes ACC′H (A = Li, F, Cl) with those of the parent molecules. In these examples the *total bonded* population $b(CC') = b_C^{C'} + b_{C'}^C$ differs by only 0.03 e over all four cases in spite of a considerable change in the separate values of $b_C^{C'}$ and $b_{C'}^C$ from the symmetrical case of HCCH. When A = Li, 0.48 e is shifted from $b_C^{C'}$ to $b_{C'}^C$, while when A = F and Cl shifts of 0.56 and 0.33 e respectively from $b_{C'}^C$ to $b_C^{C'}$ are found.

The near constancy of the nonbonded and total bonded populations as defined here is found to apply to all systems so far considered.[18] In those cases where the individual bonded populations undergo only small changes (as in FCN or CO_2), one finds that the similarity between the diatomic fragments and the triatomic systems extends beyond the population level to the actual distribution of charge in space. For example, a charge distribution for FCN obtained by discarding the nonbonded charges on C in the diatomic species $FC(X^2\Pi_r)$ and $CN(X^2\Sigma^+)$, Figure 1c, is very similar to the distribution calculated for the FCN molecule (Figure 1b).

These observations lead to the conclusion that *the extent to which properties are additive between different systems is determined by the extent to which the charge distributions of the corresponding fragments are unchanged during transfer between the systems.* This approach to the explanation of additivity, including additivity of the energy, has been discussed by Bader and Beddall.[18]

Bonds and bond properties are, of course, never completely transferable and not always approximately transferable. The major problem is to determine a partitioning scheme of a charge density, or wave function which results in quantities which properly reflect the near transferability or lack of transferability of properties between different systems. In other words

(18) R. F. W. Bader and P. M. Beddall, *Chem. Phys. Lett.*, 8, 29 (1971).

what quantities or attributes of a charge distribution or wave function make up the basic building blocks of a molecular system? The results presented here suggest that the molecular fragments as defined by planes through the nuclei may be the basic units for the understanding of additivity.

Parametrization of Semiempirical π-Electron Molecular Orbital Calculations. π Systems Containing Carbon, Nitrogen, Oxygen, and Fluorine[1]

David L. Beveridge and Juergen Hinze*

Contribution from the Department of Chemistry, University of Chicago, Chicago, Illinois 60637. *Received October 10, 1970*

Abstract: A uniform parametrization is suggested for π-electronic structure calculations of conjugated systems containing carbon, nitrogen, oxygen, and fluorine. All parameters are related directly to atomic data. The parametrization scheme is substantiated by comparing computed and observed uv spectral data and proton hyperfine coupling constants for a large number of different π-electron systems. The good correlations obtained suggest that π-electronic structure calculations, in conjunction with the proposed parametrization scheme, can be used reliably for the prediction of uv spectra and proton hyperfine coupling constants. Arguments are presented that singlet–triplet transition energies, as well as ionization potentials, cannot be predicted with equal reliability using the scheme proposed.

The application of semiempirical π-electron molecular orbital calculations to the study of chemical and spectroscopic properties of unsaturated hydrocarbons has been extensive and in general successful. The method of calculation used commonly is the semiempirical scheme of Pariser, Parr, and Pople, which is an SCF–LCAO procedure based on the independent-particle model, grossly simplified by the assumption of Σ–Π separability and the approximation of "zero differential overlap" between atomic orbitals on different centers.[2] The effect of these rather severe approximations is hopefully compensated somewhat by the introduction of semiempirical parameters into the calculation. Computations following the PPP method result in π-electron molecular wave functions, describing many important phenomena not accommodated by the simpler Hückel theory, such as separations between excited states of different multiplicity, excitation energies for electronic transitions giving rise to α and β bands in the absorption spectra of aromatic hydrocarbons, and positive as well as negative spin densities in free radicals and ions. Although computations using the PPP method are in principle no more difficult than Hückel calculations, the choice of suitable parameters for PPP calculations is more arduous, especially if hetero systems are to be treated.

Often, when π-electron calculations are performed for a limited group of similar molecules, a parametrization is effected such as to give good agreement between computed and experimental data for some molecules in the group considered. Proceeding in this manner results in a certain loss of objectivity, such as is commonly encountered in Hückel theory. In addition, it is more difficult to judge the relative reliability of calculations from different sources, when different approximations have been made in the selection of the basic parameters. If the PPP theory is general enough that it allows correlation of computed results with experimental data over a wide variety of unsaturated compounds, there must be at least one consistent choice of parameters which will yield a general and wide-reaching correlation. It is felt that there exists a need for such a unified parametrization scheme which is generally applicable, without additional modifications, to all types of atoms routinely encountered in different π-electron systems.

In order to deal with this problem we propose herein a generalized parameter scheme for PPP type calculations and detail its application to π-electron systems containing carbon, nitrogen, oxygen, and fluorine. Owing to the empirical nature of π-electron theory, it was felt that a direct theoretical parameter choice was not feasible, but the validity of an empirical parameter scheme, though derived with some theoretical reasoning, had to be demonstrated by showing its capability to predict or correlate observables. Therefore in section 3 a number of representative calculations of electronic energies and proton isotopic hyperfine coupling constants for different types of unsaturated systems are presented to substantiate the parameter scheme proposed in section 2. To clarify our notation and to avoid confusion, section 1 allows for a brief review of the π-electron formalism as it is used here.

1. Semiempirical π-Electron Theory

In the π-electron approximation the Σ part of the total electronic wave function of a molecule is assumed to be invariant to changes in the π-electron distribution and therefore considered as constant and disregarded. A molecular wave function, Ψ_s, of a stationary state, de-

(1) Research supported in part by the National Science Foundation.
(2) (a) J. A. Pople, *Proc. Phys. Soc., London, Ser. A*, **68**, 81 (1955); (b) R. Pariser and R. G. Parr, *J. Chem. Phys.*, **21**, 466, 767 (1953); (c) for additional references, see general reviews, *e.g.*, L. Salem, "The Molecular Orbital Theory of Conjugated Systems," W. A. Benjamin, New York, N. Y., 1966; K. Jug, *Theor. Chim. Acta*, **14**, 91 (1969).